Electrical and Optical Characterization of Atmospheric Pressure Co-axial Dielectric Barrier Discharge (APDBD) Used for Ozone Generation

Purna Bahadur Khadka[1], Suraj Sharma[1], Yam Prasad Basel[1], Ganesh Acharya[1], Rajendra Shrestha[2], Deepak Prasad. Subedi[3]
[1]M.sc Graduate, [2]HOD, [3]Professor
[1]Departement of Physics,
[1]Goldengate International Collage, Tribhuvan University, Kathmandu, Nepal
[2]Department of Science and Humanities, Nepal Banepa Polytechnic Institute [CTEVT], Banepa, Kavre, Nepal
[3]Department of Natural Science, Kathmandu University, Dhulikhel, Nepal.

Abstract : This work reports an experimental investigation of optical and electrical parameters of coaxial Dielectric barrier discharge (DBD) used for the production of ozone at atmospheric pressure. The discharge was produced using high voltage power supply, (0-18kV) operating at frequency of 50 Hz. The optical characterization was made by taking the spectrum of discharge by optical emission spectrometer in order to estimate the electron temperature and electron density. The electron temperature and density was estimated by line intensity ratio method and found to $1.74\times10^{17}cm^{-3}$ and 1.8eV respectively. Further, the electron density was measured by current density method and found to be $2.16\times10^{15}cm^{-3}$. In addition discharge was characterized by measuring current and voltage, which was recorded by oscilloscope in order analyze electrical parameter. The voltage was varied from (7.8kV-11kV) and gas flow rate was varied from (4.5L/min -15.5L/min) and measured by venturimeter. The energy dissipated during discharge was measured by the area of lissajous diagram, which is a plot of the charge against the discharge voltage. The obtained result showed that the energy dissipation in the system used in the present study depends on applied voltage as well as on gas flow rate.

IndexTerms **- APDBD, Electrical characterization, Lissajous diagram, Optical characterization.**

INTRODUCTION

Dielectric Barrier Discharge is auspicious approach in producing non-thermal plasma, which is widely used in variety of application [1,2,3]. Lately DBD have gathered much attention, as they are feasible and simple to construct. The application of non-equilibrium plasma produced under atmospheric pressure has been efficacious tool for biomedical application, surface modification, pollution control [4,5] etc. Recently DBD is being widely used for the production of ozone, which is use for the treatment of water [6,7]. The electrical gas discharge evolved due to high voltage in the gap between electrodes with at least one of them covered with dielectric material such as glass, quartz etc is known as dielectric barrier discharge [8]. It is also referred as silent discharge since; it does not produce any type of noise during discharge formation. The barrier placed act as a current limiter and prevents the formation of spark or an arc discharge [5].The electron density, electron temperature and power are most radical parameter in a gas discharge and plays very momentous role in understanding the discharge physic and optimization of plasma [9]. The numbers of approaches are being available to measure electron density and temperature. Some of the methods includes Languimure probe, Microwave interferometer, Laser Thomson scattering and optical emission spectroscopy (OES). Among the various method, OES technique is suitable for measurement of electron density and electron temperature [10]. Since, other method is difficult to use due to the small plasma dimension where, strong collision process in atmospheric pressure discharge takes place. The characterization of dielectric barrier discharge is very important because it allows investigation and optimization of microdischarge properties in small laboratory set up to very large-scale industrial application. The optical and electrical characterization can be investigated by measuring applied voltage, discharge current, power consumed during discharge formation, energy dissipated during discharge etc.

EXPERIMENTAL SET UP

This project aims to design of DBD reactor at atmospheric pressure for ozone generation. It consists of two cylindrical co-axial electrodes. The inner is a copper rod of 54.5 cm in length and 2.5 cm in diameter. The outer electrode is aluminum foil of 29.8 cm in length and 0.5 mm in thickness. The gap between the two electrodes is 4 mm. The borosilicate glass tube of length of 49.5 cm with external diameter and internal diameter 2.6 cm and 2.4 cm is used as barrier. The high voltage AC transformer (0-18kV, 50Hz, NEEK) was used to supply necessary voltage to the reactor. The DBD reactor consists of fourteen identical tubes in an array adjusted by the teflon. The flow rate of gas was controlled by indigenously designed venturimeter. The air blower (ALPHA, A4285, 0-50Hz, 450W, 25m 3 /min) consists of device named dimmer, which controls the flow of air in the reactor. The applied voltage to the discharge was measured using 10:1 voltage probe (Tektronix 2000TDS), and the discharge current was recorded by using a current probe. In addition digital oscilloscope was employed to obtain the voltage and current waveform. Optical emission spectra were recorded by Oceam optics (USB +2000) spectrometer for optical characterization of discharge.

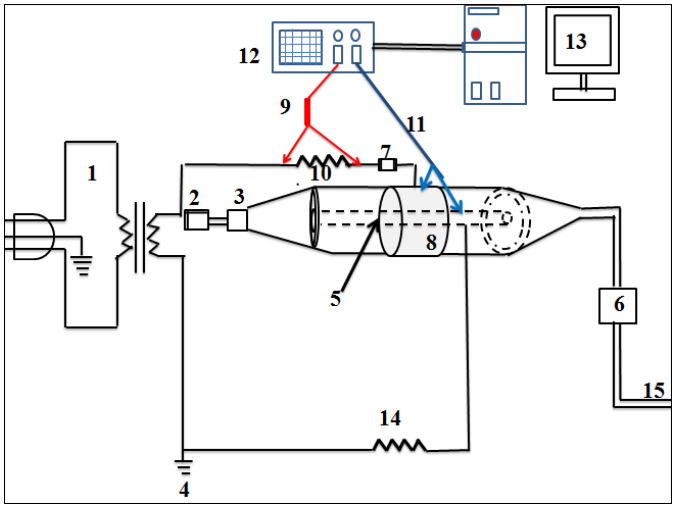

Fig.1 Schematic diagram and photograph of atmospheric pressure dielectric barrier reactor.

Where, 1=High voltage transformer, 2= Venturimeter, 3=Air blower with dimmer, 4= Ground, 5= Central electrode, 6= Ozonometer, 7= Voltage variator, 8= Ground electrode ,9= Current probe, 10= 10KΩ resistor, 11= Hight voltage probe, 12= Oscillospe, 13= Computer, 14= 5MΩ resistor.

ELECTRICAL AND OPTICAL DIGONOSTIC

Measurement of Electron temperature and electron density by Line Intesity Ratio method.

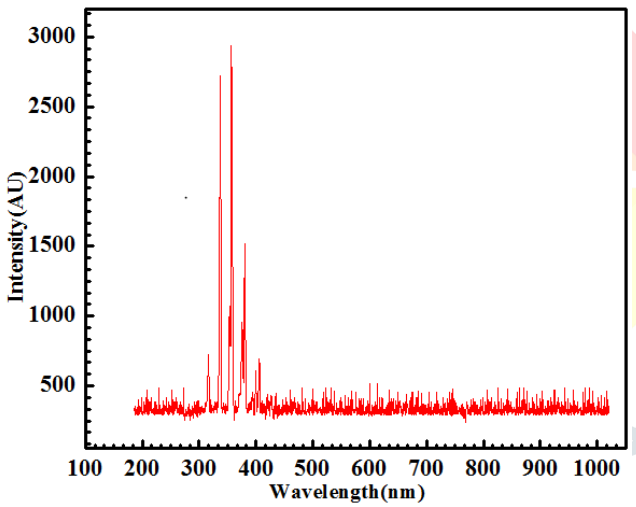

Fig.2: Optical emission spectra of atmospheric pressure discharge produced in air

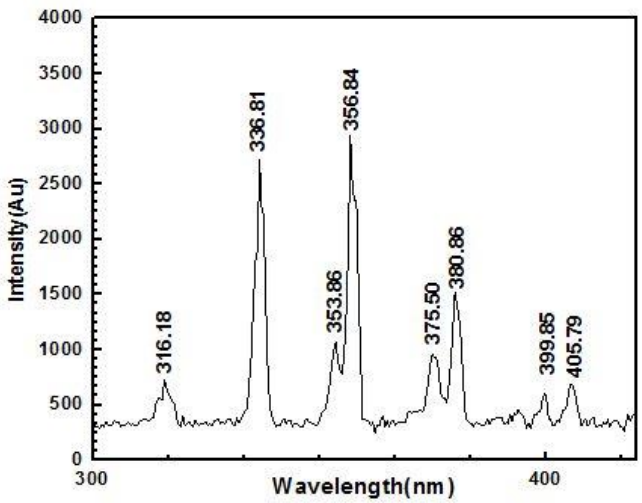

Fig.3: Optical emission spectra of atmospheric pressure discharge in the range of (300-450)nm.

Fig.2 shows the OES discharge between the wavelength 100 nm to 1100 nm with the 4mm electrode gap with applied voltage 8.31kV. The electron temperature is estimated by using the line intensity ratio method [11,12,13]. For the measurement of electron temperature, four suitable Nitrogen lines (two for NI and NII) were selected. The formula involved for the measurement of electron temperature is given by following equation (i) [14].

$$\frac{R_1}{R_2}=\frac{I_1/I_2}{I_3/I_4}=\left(\frac{A_{pq}}{A_{xy}}\right)\left(\frac{g_p}{g_x}\right)\left(\frac{A_{pq}}{A_{xy}}\right)\left(\frac{\lambda_{xy}}{\lambda_{pq}}\right)\left(\frac{A_{uv}}{A_{rs}}\right)\left(\frac{g_u}{g_r}\right)\left(\frac{\lambda_{rs}}{\lambda_{uv}}\right)\exp\left[-\frac{Ep-Ex-Er+Eu}{kTe}\right]\ldots\ldots\ldots\ldots(i)$$

Where, R is the ratio of intensity of two lines, I is the intensity of spectral lines . A_{ij} is the transition probability of the transition from i to j . g_i is the statistical weight of upper level, λ is Wavelength of radiation and E_i Energy of the upper level. T_e, Electron temperature and k is Boltzman constant.

Consider two NI lines of wavelength 600.48 nm and 746.83nm and two NII lines with wavelength 460.14nm and 499.43nm.

Table.1 Different Nitrogen lines with wavelength and intensities obtained from the recorded OES and parameters from NIST atomic spectra database [15].

Lines	Wavelength(nm)	Intensities(a.u)	A_{ij}	E(eV)	g_i	Ratio
NI	600.84	514.80	$A_{pq}=3.58\times10^{6}$	$E_p=11.60$	$g_p=2$,	I_1
NI	746.83	484.51	$A_{rs}=1.97\times10^{7}$,	$E_r=10.34$	$g_r=6$,	I_2
NII	460.14	480.01	$A_{uv}=2.22\times10^{7}$	$E_u=18.46$	$g_u=3$,	I_3
NII	499.43	469.85	$A_{xy}=2.62\times10^{7}$	$E_x=25.50$	$g_x=5$,	I_4

Using the above data in equation (i), we obtain

$$\frac{R1}{R2} = 4.17\times10^{-2} \exp\left[\frac{5.7647}{KTe}\right]$$

Table. 2: Electron temperature and corresponding intensity ratio

R_1/R_2	KT_e
1	13.31
1.3	3.52
1.6	1.53
1.6	0.87
2.2	0.58
2.5	0.42

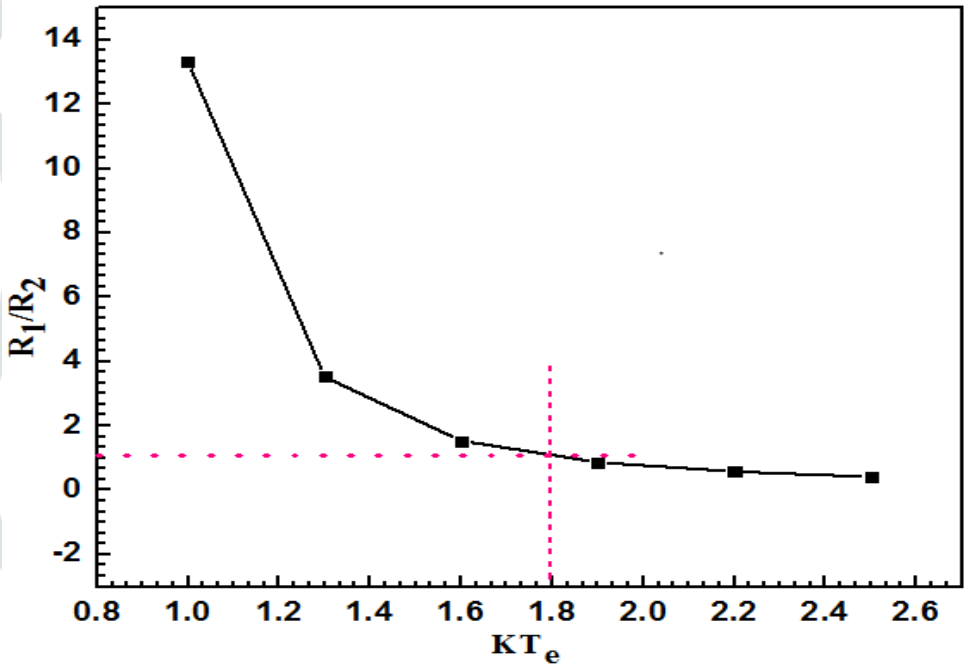

Fig.4: Plot of R_1/R_2 as a function of electron temperature (T_e).

Fig.4 is the graph plotted between Te and R_1/R_2 and used to determine the electron temperature by using value of R_1/R_2 obtained from observation. From the observation, R_1/R_2 = 1.1533 which corresponds to electron temperature1.80eV. The electron density is estimated by using line intensity ratio method and equation employed is given by equation (ii) [14,16]

$$n_e=2\left(\frac{I1}{I2}\right)\left(\frac{A_{pq}}{A_{rs}}\right)\left(\frac{g_p}{g_r}\right)\left(\frac{\lambda_{rs}}{\lambda_{pq}}\right)\left(\frac{2\pi MekTe}{h\hat{}2}\right)^{3/2}\exp-\left[\frac{Ei+Ep-Er}{kTe}\right]\ldots\ldots\ldots\ldots\text{(ii)}$$

Taking two lines NI(600.84)nm and NII(460.14)nm, the wavelength and other parameters were obtained from the NIST atomic spectra data base and intensities is obtained from the OES data recorded by spectrometer.

Table.3 Different Nitrogen lines with wavelength and intensities obtained from the recorded OES and parameters from NIST atomic spectra database [15]

Lines	Wavelength(nm)	Intensities(a.u)	A_{ij}	g_i	Ratio
NI	600.847	514.808	$A_{pq}=3.58\times10^{6}$	$g_p=2$,	I_1
NII	460.148	480.018	$A_{uv}=2.22\times10^{7}$	$g_u=3$,	I_2

Using the data from table.3 in Equation (ii) with electron temperature T_e=1.8eV and ionization potential of nitrogen 15.58eV [15], the electron density is obtained to be $1.74\times10^{17}cm^{-3}$.

Measurement of electron density by current density method.

The peak voltage and current are approximately 7.75 kV and 456mA measured by the high voltage and current probes. From the current wave we can calculate the average current density J_{ave} using relation (iii) [17,18].

$$J_{av\,e}=\frac{I}{A} \quad \text{..... (iii)}$$

where A= 2πrh is the cross sectional area of the tube, h is length of outer electrode and r is the radius of the tube.
The electron density can be estimated by current density formula given by expression

$$J = n_e\mu E \quad \text{..... (iv)}$$

where, e is the elementary charge. For the electron mobility we use $\mu = 3 \times 10^{-2}$ m ^{2}/V [16], the strength of the electric field E = ΔV/D is calculated by taking ΔV = V, i.e. the voltage drop equals the amplitude. D is the distance between the electrodes. In our experiment we use r=2.4cm, h=29.8cm, D=4mm

$E = \frac{V}{D} = 1.94\times10^{6}Vm^{-1}$

$A = 2.25\times10^{-2}m^2$

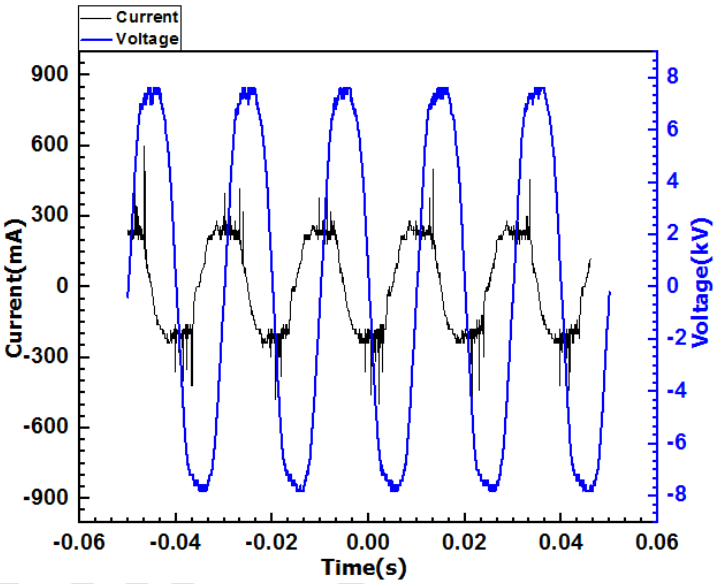

Fig 5: Characteristics I-V curve with applied voltage 8.31kV.

Using these values in equation (iv) the electron density was calculated and found to be $n_e = 2.163\times10^{15}cm^{-3}$.

Energy dissipation during discharge

The key parameter for measuring the efficiency of the device is energy consumed per cycle. During the optimization of the device into large-scale installation, study of energy consumption by the device is required. The plot between the charge transferred and input voltage is responsible for the calculation of the energy, which is injected to the gas during the discharge. The plot between the charge (Q) and input voltage (V) is called the lissajous figure. The area enclosed by the lissajous figure determines the energy dissipated during a complete cycle[19,20].

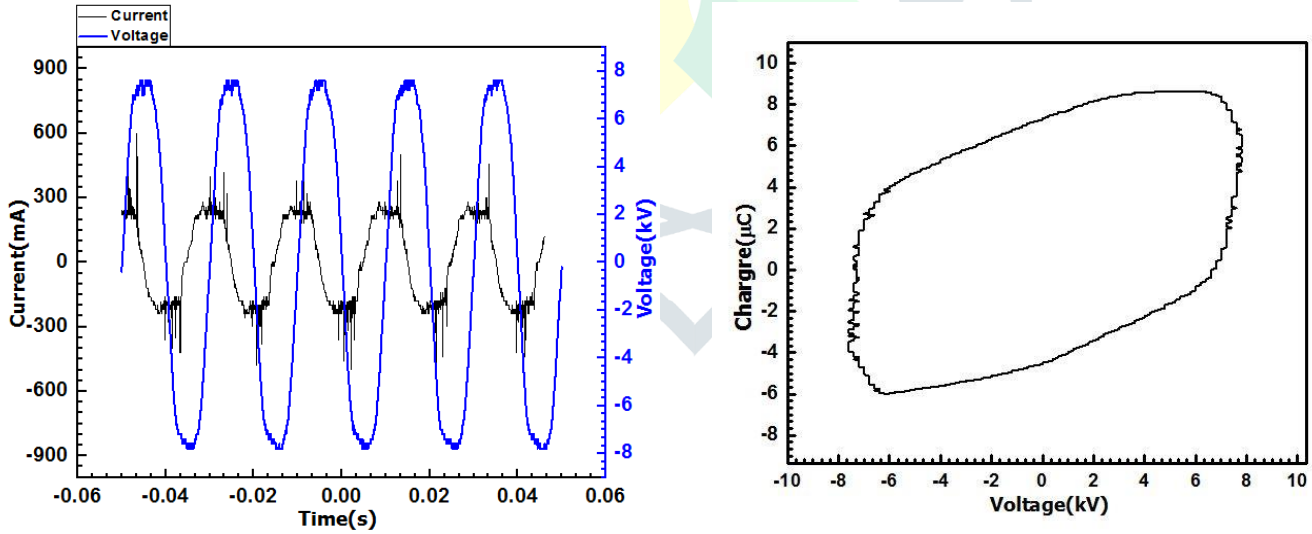

Fig.6: Characteristics I-V curve and Lissajous figure at applied voltage 8.31kV.

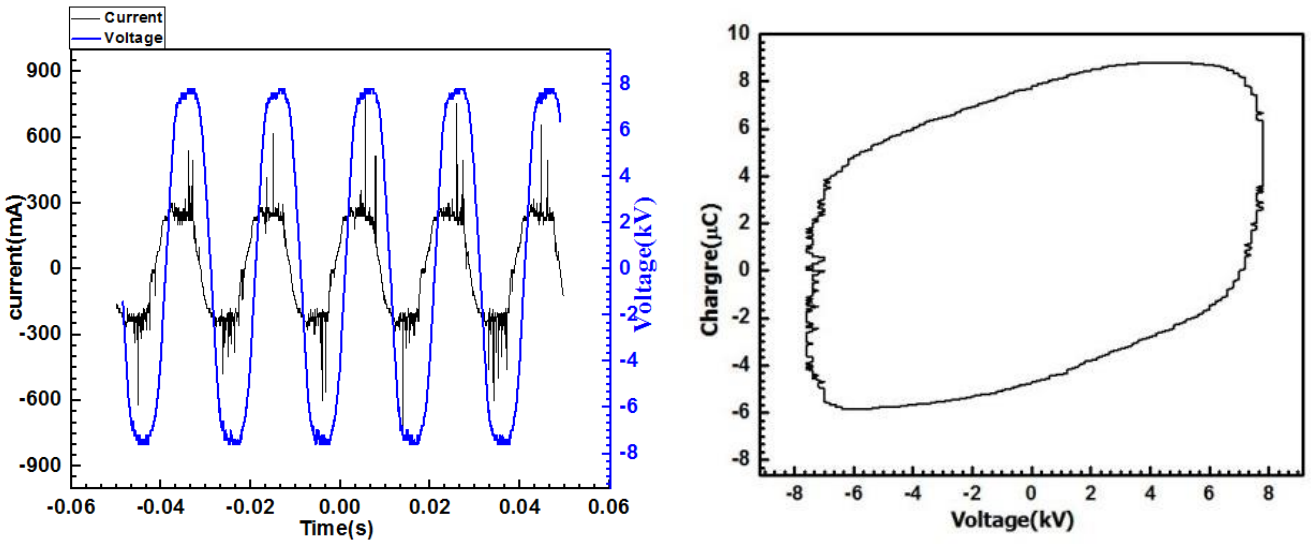

Fig.7: Characteristics I-V curve and Lissajous diagram with applied voltage 8.84kV.

Fig. 6 and Fig. 7 shows the characteristics I-V curve and Lissajous diagram at applied voltage 8.31kV and 8.84kV respectively. Additionally, similar trend is followed for other applied voltage and gas flow rate.

Effect of applied voltage on dissipated energy

In filamentary mode plasma formation, conductive channels are restricted to form the microdischarge. The non-ionized gas present between the gaps serves as background a reservoir to absorb the energy dissipated in the microdischarge collect and transport to the long-lived species, which are created in the plasma. The total charge transfer in the microdischarge depends on the gas properties, flow rate of gas, applied voltage; it is influenced by the gap spacing and by the properties of dielectric material placed as a barrier. The discharge starts even at the small-applied voltage but at this condition significant amount charge cannot be transferred. When the voltage is increased the charge transfer to the gas increases this is due fact that applied voltage causes the breakdown [1]. When the applied voltage is sufficient for the discharge, the charge during the discharge is accumulated on the dielectrics, which reduce the electric field and consequently quenching of the discharge filament takes place. Higher the applied voltage higher is electric field that increases the chances of electron impact [21].

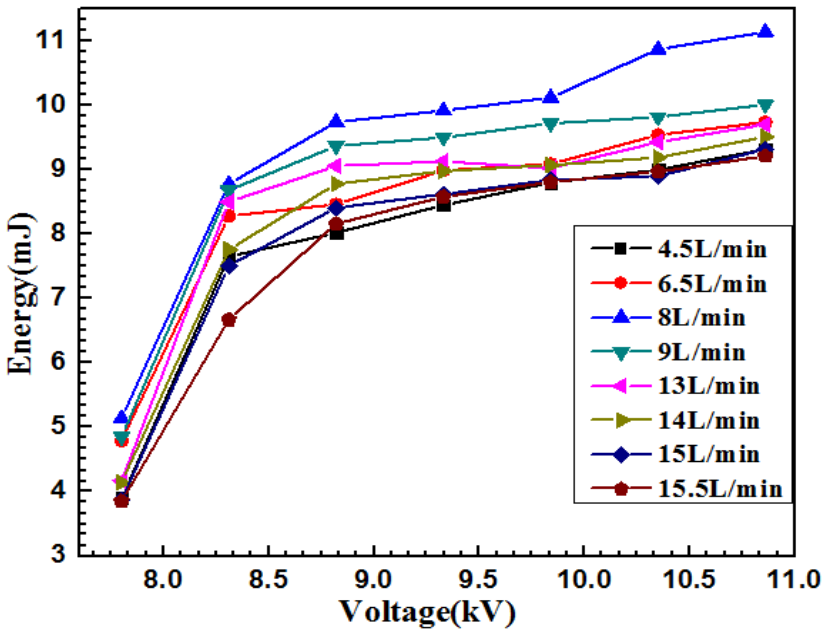

Fig.8: Evolution of energy dissipated as the function of applied voltage with varied airflow rate.

The evolution of the dissipated energy per cycle as function of applied voltage with gas flow rate from 4.5 l/min to 15.5 l/min is shown in Fig.8. The figure revels that electrical energy increases as the applied voltage increases. It is due to the fact that, increasing the applied voltage increases the number of microdischarge consequently the rate of reaction increases and more excited species and radicals along with other particles increases. The increase in the plasma filament leads to increase in the charge transfer from very high reactive electron to the gas and results to increase in the energy injected to the gas present between the gap. The transported charge increases non linearly with increase in applied voltage. Greater the amount of transported charge result in higher plasma reaction and causes greater discharge energy [22]. As the voltage is increased, the energy dissipated to the dielectric barrier discharge increases. The increase in energy is due to increase in surface resistance, which cause to increase in the energy consumed during the charge transfer from the discharging region to the non-discharging region [22,23]. As voltage increases, the number of microdischarge increases and hence discharge current increases which increase the transported charge and results to increase the dissipated energy. An increase of the electric field strength in the air gap of the reactor may lead to increase in the discharge intensity and increase of microdischarge channel in the discharge space. This results more charge transfer in the space, which consequently increases the dissipated energy.

Effect of gas flow rate on dissipated energy.

From Fig 9, it is evident that there exists a value of flow rate at which the energy dissipation is maximum. Moreover, the value of flow rate, at which the energy dissipation is maximum, is different for different applied voltages. As it can be seen from Fig.9 the energy dissipation is maximum with the flow rate 4.5 l/min with applied voltage 7.8 kV. However, the maximum energy with the applied 8.31kV and 8.84kV is at 6.5L/min. Figure clearly shows that maximum energy consumed during the discharge formation for the production of ozone is 8l/min with applied voltage 9.33kV and 9.84kV. In addition, the maximum energy dissipated during the discharge formation with applied voltage 10.35kV and 10.86kV is 9l/min.

The increase in dissipated energy per cycle with gas flow rate is due to the following reason; when the gas flow rate is increased rate of collision between the electron and gas atoms increases. The collision plays a vital role to build up reactive species by step ionization mechanism. The reactive species generated within the plasma during the discharge formation plays a key role to transfer the charge during collision between electron and gas atoms. The increased charge transfer increases the dissipated energy with rise in flow rate, since the charge transfer is proportional to dissipated energy.

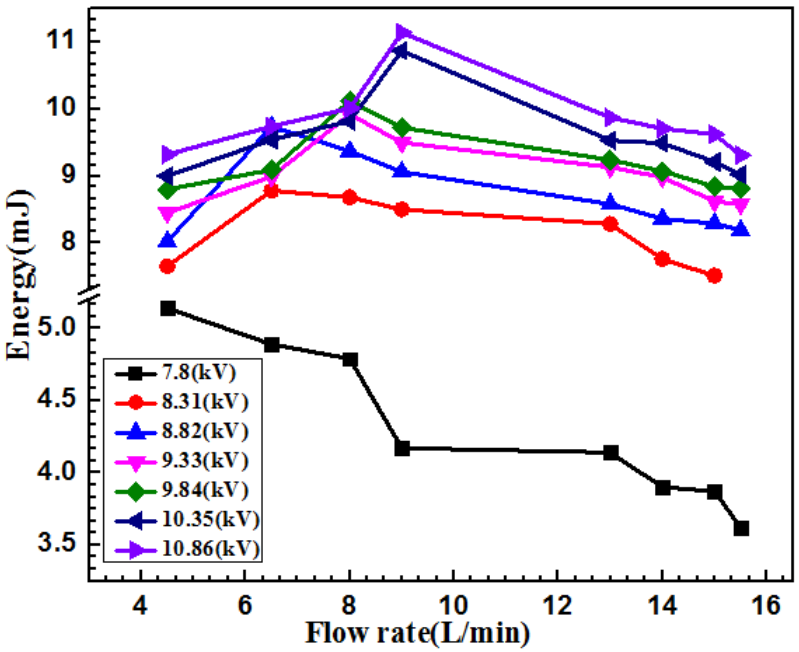

Fig.9: Variation of energy dissipated as the function of airflow rate with varied applied voltage.

However, rise in flow rate higher then certain flow rate, the applied voltage ionizes less number of gas atom lowering the number of reactive species within the electrode gap. On the other hand, decrease in dissipated energy may due to smaller residence time of gas molecules within the discharge gap and coiling effect. As a result, collision rate between the gas atoms and electrons falls down resulting less number of charge transfer. So the decrease in dissipated energy is observed with higher gas flow rate.

CONCLUSION

In this work, a co-axial dielectric barrier discharge plasma device with 4mm electrode gap at atmospheric pressure has been built up in order to generate ozone. The optical and electrical parameters of the device such as electron temperature, electron density and dissipated energy have been determined. The electron density (n_e) is determined by line intensity ratio method and by current density electrical method. The electron density (n_e) and electron temperature determined by line intensity ratio method have been found to be $1.74\times10^{17}cm^{-3}$ and 1.8eV, whereas the electron density by electrical method has found to be $2.163\times10^{15}cm^{-3}$. For measuring the dissipated energy, procedure is based on Lissajous curve obtained by plotting charge against voltage i.e (Q-V) curve. The area inside the closed Lissajous curve have been calculated to obtained energy consumed per cycle during discharge formation. The effect of applied voltage and gas flow rate on the dissipated energy has been investigated. It is concluded that the dissipated energy increased with increase of applied voltage. Similarly, variation of dissipated energy per cycle as a function of gas flow rate was observed and it was found that there exists a value of flow rate at which the energy dissipation is maximum. Moreover, further rise in gas flow rate decreases the dissipated energy during discharge.

REFERENCES

[1] U. Kogelschatz, B. Eliasson and W. Egli**,** Dielectric-Barrier Discharges. Principle and applications, Le Journal de Physique IV, 7 : (C4-47), 1997

[2] G. Borcia, C. A Anderson, N. M. D Brown, The Surface Oxidation of Selected Polymers Using an Atmospheric Pressure air Dielectric Barrier part I, Surface Science , 221, 203 (2004)

[3] Nagaraj, Gayathri and Balasubramanian, Manjula and Kalghatgi, Sameer and Wu, Andrew S and Brooks, Ari D and Fridman, Gregory and Cooper, Moogega and Vasilets, Victor N and Gutsol, Alexander and Fridman, Alexander, IEEE, 35, 1559 – 1566, 2007

[4] U. Kogelschatz, B. Eliasson, W. Egli, From Ozone Generators to Flat Television Screens: History and Future Potential of Dielectric-Barrier Discharges, Pure and Applied Chemistry , 71, 1819 (1999)

[5] Pietsch, Gerhard J and Gibalov, Valentin I, Dielectric Barrier Discharges and Ozone Synthesis,Pure and Applied Chemistry,70, 1998, (1169-1174)

[6] Magara, Y and Itoh, M and Morioka, T, Application of Ozone to Water Treatment and Power Consumption of Ozone Generating Systems, Progress in Nuclear Energy, 29, 175—182 ,(1995)

[7] U. N. Pal, M. Kumar, H. Khatun, A. K. Sharma, Discharge characteristics of dielectric barrier discharge (DBD) based VUV/UV sources, J. Phys Conference Series,114, 1 (2008)

[8] Becker K H, Kogelschatz U, K H Schoenbach & Barker R J, Non-equilibrium Air Plasma at Atmospheric pressure. IOP, University of reading, Berkshir, (2005).

[9] U. Kogelschatz , Dielectric-Barrier Discharges: Their History, Discharge Physics, and Industrial Applications, Plasma Chemistry and Plasma Processing , 23, 1 (2003)

[10] Zhu X M, Pu Y K, Balcon N & Baswell R,. The Spatial--Temporal Evolution of the Electron Density and Temperature for a Nanosecond Microdischarge,J Phys D; Appl Phys, 42 -142003 (2009)

[11] D. P Subedi, R. B Tyata, R. Shrestha, C. S Wong , An Experimental Study of Atmospheric Pressure Dielectric Barrier Discharge (DBD) in Argon, AIP Conference , 1588,103 (2014).
[12] A. A Kadhim, A. A Abdalameer, N. K. Tawfeeq, A. Hasan, H. H Murbat, Electron temperature and density measurement of plasma jet in atmospheric pressure, Int.J. Phy. Chem. and Math., 2, 28 (2007)
[13] Chen F F, Introduction to Plasma Physics and Controlled fusion 2nded. New York (1984).
[14] Balcon, Nicolas and Aanesland, Ana and Boswell, Rod, Pulsed RF Discharges, Glow and Filamentary mode at Atmospheric Pressure in Argon, Plasma Sources Science and Technology, 16, 2007,(217)
[15] https://physics.nist.gov/PhysRefData/ASD/lines_form.html
[16] R. Shrestha1 D.P Subedi1, B.K. Shrestha ,A. Shrestha1, Surface Modification of Polypropylene by Atmospheric Pressure Cold Argon/Oxygen Plasma Jet, International Journal of Recent Research and Review, IX, 2016
[17] A. Sarani, A. Nikiforov, and C. Leys. Atmospheric Pressure Plasma jet in Ar and Ar/H 2 O mixtures: Optical Emission Spectroscopy and Temperature Measurement, Physics of Plasmas, 17(6):8, (2010)
[18] B. Eliasson,U. Kogelschatz, Modeling and Applications of Silent Discharge Plasmas, IEEE transactions on plasma science, 19, 309 (1991)
[19] W. H Tay, S.L Yap, C.S Wong, Role of Secondary Emission on Discharge Dynamics in an Atmospheric Pressure Dielectric Barrier Discharge, Sains Malaysiana, 43, 583 (2014)
[20] Pal, UN and Kumar, M and Khatun, H and Sharma, AK, Discharge characteristics of dielectric barrier discharge (DBD) based VUV/UV sources, Journal of Physics: Conference Series,144, 012065, (2008)
[21] Wang, Xiaojing and Yang, Qing and Yao, Chenguo and Zhang, Xiaoxing and Sun, Caixin, Molecular Diversity Preservation International,4 ,2011, (2133-2150).
[22] I. Biganzoli, R. Barni, A. Gurioli, R. Pertile, C. Riccardi, Dielectric Barrier Discharge Characteristics of Multineedle-to-Cylinder Configuration,Journal of Physics: Conference Series , 0550, 012039 (2014)
[23] Shahbazi Rad, Zahra and Abbasi Davani, Fereydoun, Experimental Investigation on Electrical characteristics and dose measurement of dielectric barrier discharge plasma device Used for Therapeutic Application AIP, 88, 2017, (043504)